Hindawi
Advances in Materials Science and Engineering
Volume 2019, Article ID 8751540, 9 pages
https://doi.org/10.1155/2019/8751540

Research Article

Sealing Performance of Bionic Striped Mud Pump Piston

Qian Cong,[1] Tianyu Gao,[1] Yiwen Sun,[2] and Weijun Tian[1]

[1]*Key Laboratory of Bionic Engineering (Ministry of Education, China), Jilin University, Changchun 130022, China*
[2]*HiRain Technologies Co., Ltd., Beijing 100191, China*

Correspondence should be addressed to Weijun Tian; tianweijun@jlu.edu.cn

Received 13 October 2018; Revised 8 December 2018; Accepted 15 January 2019; Published 4 February 2019

Academic Editor: Antonio Caggiano

The mud pump piston is a key part for providing mud circulation, but its sealing performance often fails under complex working conditions, which shorten its service life. Inspired by the ring segment structure of earthworms, the bionic striped structure on surfaces of the mud pump piston (BW-160) was designed and machined, and the sealing performances of the bionic striped piston and the standard piston were tested on a sealing performance testing bench. It was found the bionic striped structure efficiently enhanced the sealing performance of the mud pump piston, while the stripe depth and the angle between the stripes and lateral of the piston both significantly affected the sealing performance. The structure with a stripe depth of 2 mm and angle of 90° showed the best sealing performance, which was 90.79% higher than the standard piston. The sealing mechanism showed the striped structure increased the breadth and area of contact sealing between the piston and the cylinder liner. Meanwhile, the striped structure significantly intercepted the early leaked liquid and led to the refluxing rotation of the leaked liquid at the striped structure, reducing the leakage rate.

1. Introduction

Mud pumps are key facilities to compress low-pressure mud into high-pressure mud and are widely used in industrial manufacture, geological exploration, and energy power owing to their generality [1–4]. Mud pumps are the most important power machinery of the hydraulic pond-digging set during reclamation [5] and are major facilities to transport dense mud during river dredging [6]. During oil drilling, mud pumps are the core of the drilling liquid circulation system and the drilling facilities, as they transport the drilling wash fluids (e.g., mud and water) downhole to wash the drills and discharge the drilling liquids [7–9]. The key part of a mud pump that ensures mud circulation is the piston [10, 11]. However, the sealing of the piston will fail very easily under complex and harsh working conditions, and consequently, the abrasive mud easily enters the kinematic pair of the cylinder liner, abrading the piston surfaces and reducing its service life and drilling efficiency. Thus, it is necessary to improve the contact sealing performance of the mud pump piston.

As reported, nonsmooth surface structures can improve the mechanical sealing performance, while structures with radial labyrinth-like or honeycomb-like surfaces can effectively enhance the performance of gap sealing [12–14]. The use of nonsmooth structures into the cylinder liner friction pair of the engine piston can effectively prolong the service life and improve work efficiency of the cylinder liner [15–17]. The application of nonsmooth grooved structures into the plunger can improve the performance of the sealing parts [18, 19]. The nonsmooth structures and sizes considerably affect the sealing performance [20]. Machining a groove-shaped multilevel structure on the magnetic pole would intercept the magnetic fluid step-by-step and slow down the passing velocity, thus generating the sealing effect [21–23]. Sealed structures with two levels or above have also been confirmed to protect the sealing parts from hard damage [24]. The sealing performance of the high-pressure centrifugal pump can be improved by adding groove structures onto the joint mouth circumference [25]. The convex, pitted, and grooved structures of dung beetles, lizards, and shells are responsible for the high wear-resistance, resistance reduction, and sealing performance [26–28]. Earthworms are endowed by wavy nonsmooth surface structures with high resistance reduction and wear-resistance ability [29]. The movement of earthworms in the living environment is very

similar to the working mode of the mud pump piston. The groove-shaped bionic piston was designed, and the effects of groove breadth and groove spacing on the endurance and wear-resistance of the piston were investigated [30]. Thus, in this study, based on the nonsmooth surface of earthworms, we designed and processed a nonsmooth striped structure on the surface of the mud pump piston and tested the sealing performance and mechanism. This study offers a novel method for prolonging the service life of the mud pump piston from the perspective of piston sealing performance.

2. Design and Tests

2.1. Design and Processing of Bionic Striped Piston. The BW-160 mud pump with long-range flow and pressure, small volume, low weight, and long-service life was used here. The dimensions and parameters of its piston are shown in Figure 1.

A striped structure was designed and processed on the contact surface between the piston cup and the cylinder liner. The striped structure was 5 mm away from the outermost part of the lip, which ensured the lip could contact effectively with the cylinder liner. Based on the structural dimensions of the piston cup, we designed a 2-stripe structure, and the very little stripe space affected the service life of the piston [30]. Thus, the stripe space of our bionic piston was set at 5 mm. According to the machining technology, two parameters of stripe depth h and the angle between the stripes and lateral of the piston α were selected (Figure 2).

2.2. Mud Pump Piston Sealing Performance Test. A mud pump piston sealing performance test bench was designed and built (Figure 3). This bench mainly consisted of a compaction part and a dynamic detection part. The compaction part was mainly functioned to exert pressure, which was recorded by a pressure gauge, to the piston sealed cavity. This part was designed based on a vertical compaction method: after the tested piston and the sealing liquid were installed, the compaction piston was pushed to the cavity by revolving the handle. Moreover, the dynamic detection part monitored the real-time sealing situation and was designed based on the pressure difference method for quantifying the sealing performance. This part was compacted in advance to the initial pressure P_0 (0.1 MPa). After compaction, the driving motor was opened, and the tested piston was pushed to drive the testing mud to reciprocate slowly. After 1 hour of running, the pressure P on the gauge was read, and the pressure difference was calculated as $\Delta P = P_0 - P$, which was used to measure the sealing performance of the piston.

To more actually simulate the working conditions of the mud pump, we prepared a mud mixture of water, bentonite (in accordance with API Spec 13A: viscometer dial reading at 600 r/min ≥ 30, yield point/plastic viscosity radio ≤ 3, filtrate volume ≤ 15.0 ml, and residue of diameter greater than 75 μm (mass fraction) ≤ 4.0%), and quartz sand (diameter 0.3–0.5 mm) under complete stirring, and its density was 1.306 g/cm^3 and contained 2.13% sand.

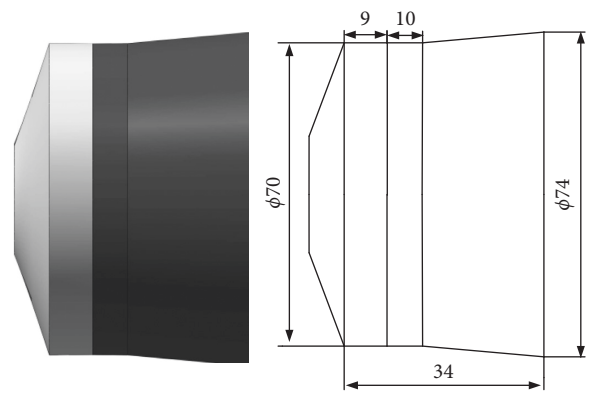

Figure 1: Standard piston and its dimensions (mm).

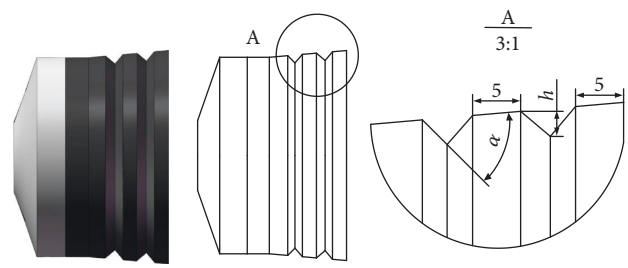

Figure 2: Striped piston and its structure and its dimensions (mm).

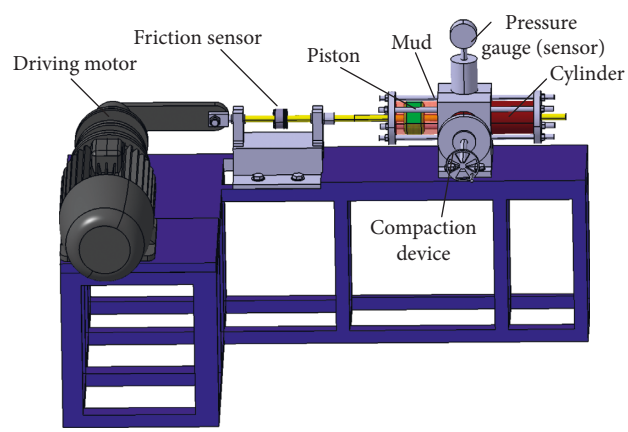

Figure 3: Mud pump piston seal test bench.

3. Tests and Result Analysis

3.1. Sealing Performance Tests. The orthogonal experimental design method was used to study the effect of factors and the best combination of factor levels [31]. Stripe depth h and angle α were selected as the factors and were both set at three levels in the sealing performance tests (Table 1).

The test index was the percentage of sealing performance improvement β calculated as

$$\beta = \left(\frac{\Delta P_1 - \Delta P_2}{\Delta P_1}\right) \times 100\%, \quad (1)$$

where ΔP_1 and ΔP_2 are the pressure differences after the runs with the standard and the bionic pistons, respectively (ΔP_1 = 0.076 MPa).

Table 1: Factors and levels.

Level	Stripe depth h (mm)	Angle α (°)
1	1	45
2	2	60
3	3	90

The experimental scheme and results were listed in Table 2.

The sealing performance tests showed the striped structures all effectively enhanced the contact sealing between the piston and the cylinder liner. In particular, the increase of sealing performance relative to the standard piston minimized to 21.05% in the bionic striped piston with a stripe depth of 3 mm and angle of 45° and maximized to 90.79% in the bionic striped piston with the stripe depth of 2 mm and angle of 90°. Range analysis showed the sealing performance of pistons was affected by the stripe depth h and angle α, and these two parameters (h and α) have the same effect on the sealing performance.

Figure 4 shows the effects of stripe depth and angle on the sealing performance of mud pump pistons. Clearly, the stripe depth should be never too shallow or deep, while a larger angle would increase the sealing performance more (Figure 4).

3.2. Sealing Validity Tests. Sealing validity tests were conducted to validate the sealing performance of the bionic striped pistons. It was observed whether the sealing liquid would leak at the tail of the cylinder liner, and the time of leakage was recorded. The standard piston and the most effective bionic piston were selected to compare their sealing performances.

Both the standard piston and the bionic striped piston leaked, which occurred after 84 and 249 minutes of operation, respectively (Figure 5). Figure 6 shows the pressures of the two pistons during testing. Clearly, the sealing pressure of the standard piston declined rapidly before the leakage, but that of the bionic piston decreased very slowly. After the leakage, the reading on the pressure gauge in the standard piston declined to 0 MPa within very short time, but that of the bionic piston decreased much more slowly.

The beginning time of leakage was inconsistent between the standard and bionic pistons (84 minutes vs. 249 minutes). In order to compare the leakage of these two pistons, the leaked liquid was collected when the piston started to leak. The volume of the leaked liquid was measured using a graduated cylinder every 5 minutes from the 84th minute and 249th minute, respectively (both considered as 0 minute), for 20 minutes. Figure 7 shows the leaked amounts of the standard piston and the bionic piston. Clearly, after the leakage and failure, the leaking speed and amount of the bionic piston were both smaller than those of the standard piston.

4. Sealing Mechanism of the Bionic Striped Piston

4.1. Finite Element Numerical Simulation and Sealing Mechanism. The piston lips and the cylinder liner were under interference contact, and their mutual extrusion was

Table 2: Experimental scheme and results.

Factor test	Stripe depth h (mm)	Angle α (°)	Pressure differences ΔP_2 (MPa)	Increased rate of sealing β (%)
1	1	45	0.044	42.11
2	1	60	0.027	64.47
3	1	90	0.014	81.58
4	2	45	0.021	72.37
5	2	60	0.022	71.05
6	2	90	0.007	90.79
7	3	45	0.060	21.05
8	3	60	0.034	55.26
9	3	90	0.030	60.53
$\overline{y}_{j1}$	62.72	45.18		
$\overline{y}_{j2}$	78.07	63.59		
$\overline{y}_{j3}$	45.61	77.63		
R_j	32.46	32.46		

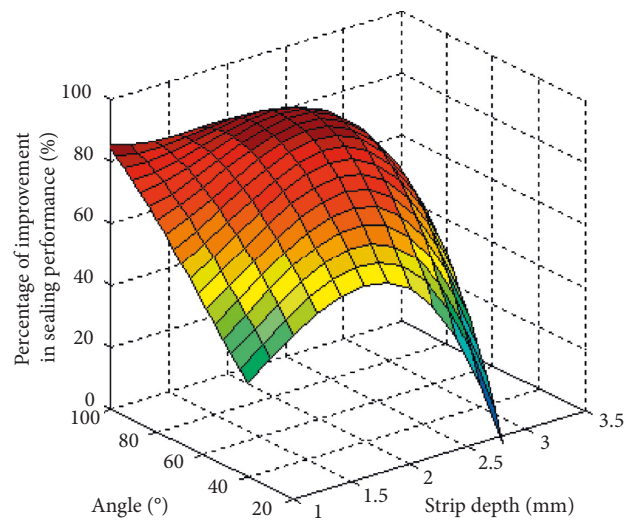

Figure 4: Influence of the striped structure on sealing performance of the mud pump piston.

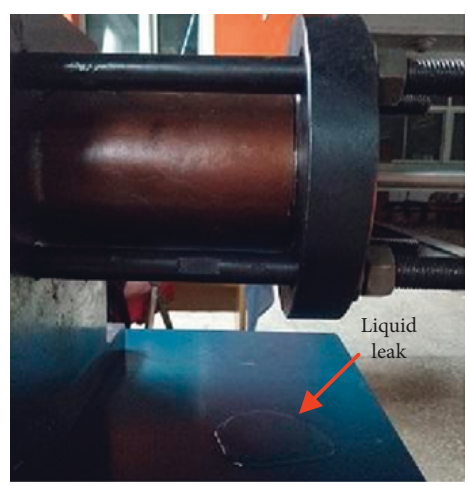

Figure 5: Leakage of sealing liquid.

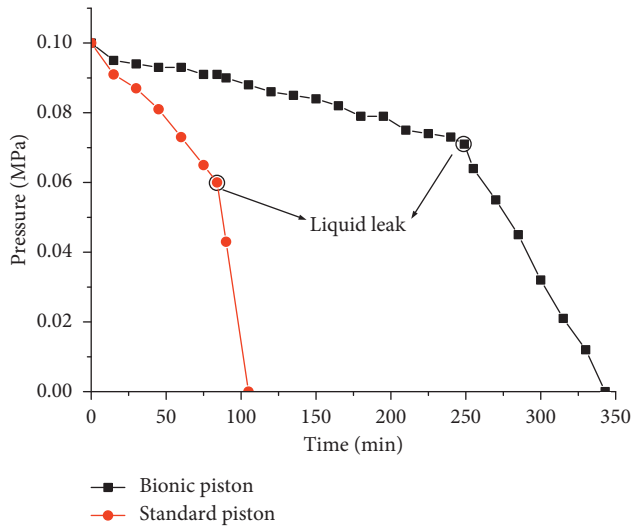

Figure 6: The pressure changes during the operations of the pistons.

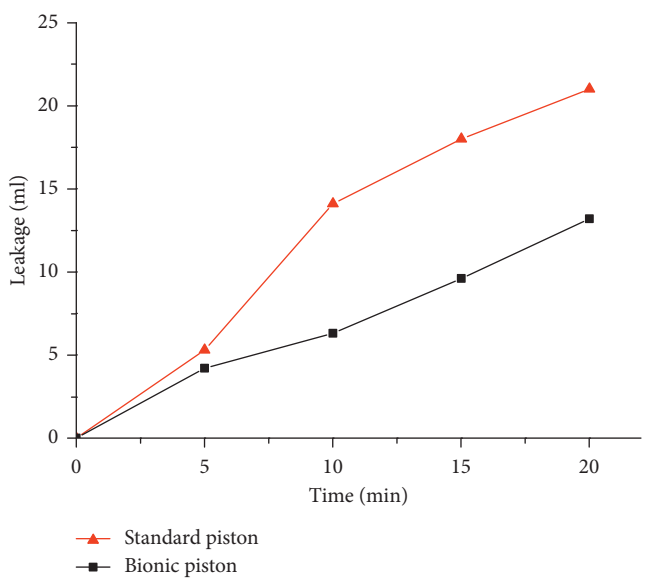

Figure 7: Leaked amounts of the pistons.

responsible for the lip sealing. Thus, a larger pressure between the piston lips and the cylinder liner reflects a higher lip sealing effect.

The bionic striped piston with the highest sealing performance ($h = 2$ mm, $\alpha = 90^\circ$) was selected for the sealing mechanism analysis and named as the bionic piston. The 3D point cloud data of standard piston were acquired by using a three-dimensional laser scanning system (UNIscan, Creaform Inc., Canada). Then, the standard piston model was established by the reverse engineering technique. The striped structure of the bionic piston was modeled on basis of the standard piston.

4.1.1. Contact Pressure of Piston Surface. The standard piston and the bionic piston were numerically simulated using the academic version of ANSYS® Workbench V17.0. Hexahedral mesh generation method was used to divide the grid, and the size of grids was set as 2.5 mm. The piston grid division is shown in Figure 8, and the grid nodes and elements are shown in Table 3. The piston cup was made of rubber, which was a hyperelastic material. A two-parameter Mooney–Rivlin model was selected, with $C_{10} = 2.5$ MPa, $C_{01} = 0.625$ MPa, $D_1 = 0.3$ MPa^{-1}, and density $= 1120$ kg/m^3 [32, 33]. The loads and contact conditions related to the piston of the mud pump were set. The surface pressure of the piston cup was set as 1.5 MPa, and the displacement of the piston along the axial direction was set as 30 mm. The two end faces of the cylinder liner were set as "fixed support," and the piston and cylinder liner were under the frictional interfacial contact, with the friction coefficient of 0.2.

Figure 9 shows the pressure clouds of the standard piston and the bionic piston. Since the simulation model was completely symmetrical and the pressures at the same position of each piston were almost the same, three nodes were selected at the lip edge of each piston for pressure measurement, and the average of three measurements was used as the lip edge pressure of each piston. The mutual extrusion between piston and cylinder liner happened at the lip, and thereby the larger of the lip pressure was, the better the sealing performance was. The lip pressure of the standard piston was smaller than that of the bionic piston (2.7371 ± 0.016 MPa vs. 3.0846 ± 0.0382 MPa), indicating the striped structure enhanced the mutual extrusion between the bionic piston and the cylinder liner and thereby improved the sealing performance between the lips and the cylinder liner. As a result, sand could not easily enter the piston-cylinder liner frictional interface, which reduced the reciprocated movement of sand and thereby avoided damage to the piston and the cylinder liner.

Figure 10 shows the surface pressures from the lip mouth to the root in the standard piston and the bionic piston. The surface pressure of the bionic piston surpasses that of the standard piston, and the pressure at the edge of each striped structure changes suddenly: the pressures at the striped structure of the bionic piston are far larger than at other parts. These results suggest the contact pressure between the edges of the striped structures and the cylinder liner is larger, and the four edges of the two striped structures are equivalent to a four-grade sealed lip mouth formed between the piston and the cylinder liner, which generates a multilevel sealing effect and thereby largely enhances the sealing effect of the piston.

4.1.2. Leakage Flow Field of Piston Surface. The piston surface flow field was numerically simulated using the CFX module of the software ANSYS® Workbench V17.0. The side of the lips was set as fluid inlet, and the other side as fluid outlet, as shown in Figure 11. The inlet and outlet were set as opening models, and the external pressure difference between them was 0 Pa. The moving direction of the piston was opposite to the fluid flow direction. The fluid region was divided into grids of 0.2 mm, while the striped structures were refined to grade 2.

Figures 12 and 13 show the surface streamline clouds and sectional streamline clouds of the two pistons at the early

(a) (b)

Figure 8: Piston grid division: (a) standard piston; (b) bionic piston.

Table 3: Grid nodes and elements.

Piston	Node	Element
Standard piston	99819	60805
Bionic piston	109689	67447

stage of leakage when the fluid entered the interface. Clearly, compared with the standard piston, when the surface-leaked liquid from the bionic piston passed the striped structure, the streamlines were sparse and significantly decreased in number, and the flow velocity declined more. The flow velocity decreased from 0.9348 m/s to 0.7555 m/s in the bionic piston and from 0.9346 m/s to 0.9262 m/s in the standard piston. It shows that, after the blockage by the striped structures, the striped structure more significantly intercepted the leaked liquid and could reduce the leakage rate of the piston, thereby enhancing the sealing effect.

Figure 13 shows the section leakage streamline of the standard piston and the bionic piston. Clearly, compared with the standard piston, when the leaked liquid of the bionic piston flowed through the striped structures, the streamlines would reflux and reverse inside the striped structures, indicating the striped structures can efficiently store the leaked liquid and slow down the leakage.

4.2. Observation of Sealed Contact of Pistons and Sealing Mechanism. To better validate the sealing mechanism of the bionic striped pistons, a piston's performance testing platform was independently built and the sealed contact of the pistons was observed. A transparent toughened glass cylinder liner was designed and machined. The inner diameter and the assembly dimensions of the cylinder liner were set according to the standard BW-160 mud pump cylinder liners. The sealing contact surfaces of the pistons were observed and recorded using a video recorder camera.

Figure 14 shows the surface contact of the standard piston and the bionic piston. Clearly, in the contact areas between the standard piston and the cylinder liner, only the narrow zone at the lip mouth contacted, as the contact width was only 4.06 mm. On the contrary, the contact areas between the bionic piston and the cylinder liner were all very wide, as the contact width was about 18.36 mm, and the sealed area was largely enlarged (892.8 mm^2 vs. 4037.6 mm^2) according to the contact areas calculated, which were favorable for improving the sealing performance.

Figure 15 shows the oil film left after the piston running. The oil film width of the bionic piston was far larger than that of the standard piston (20.48 mm vs. 2.28 mm). The striped structure of the bionic piston could store the lubricating oils, and uniform oil films were formed after its repeated movement, which reduced the friction between the piston and the cylinder liner, so that the seal failure of the piston would not happen due to excessive abrasion.

5. Conclusions

(1) The bionic striped structure significantly enhanced the sealing performance of the mud pump pistons. The stripe depth and the angle between the stripes and the piston were two important factors affecting the sealing performance of the BW-160 mud pump pistons. The sealing performance was enhanced the most when the stripe depth was 2 mm and the angle was 90°.

(2) The bionic striped structure can effectively enhance the contact pressure at the piston lips, enlarge the mutual extrusion between the piston and the cylinder liner, reduce the damage to the piston and cylinder liner caused by the repeated movement of sands, and alleviate the abrasion of abrasive grains between the piston and the cylinder liner, thereby largely improving the sealing performance.

(3) The bionic striped structure significantly intercepted the leaked liquid, reduced the leakage rate of pistons, and effectively stored the leaked liquid, thereby reducing leakage and improving the sealing performance.

(4) The bionic striped structure led to deformation of the piston, enlarged the width and area of the sealed contact, the stored lubricating oils, and formed

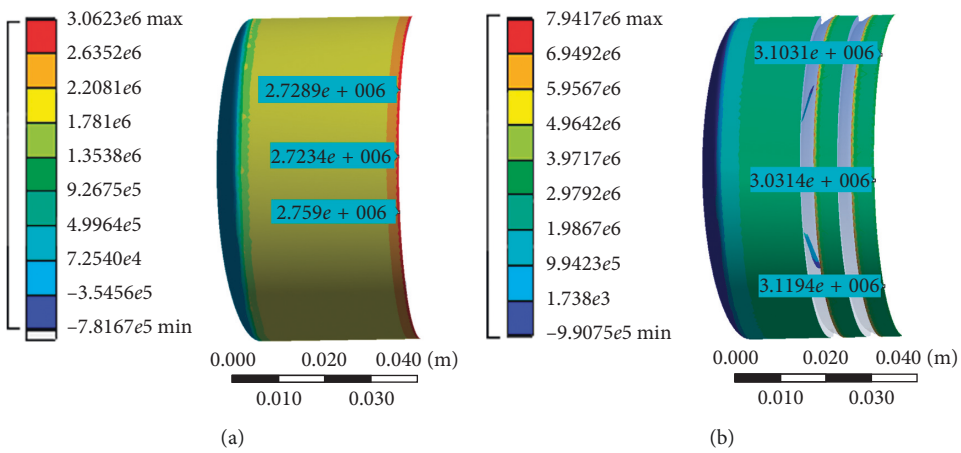

Figure 9: The pressure cloud at piston lips: (a) standard piston; (b) bionic piston.

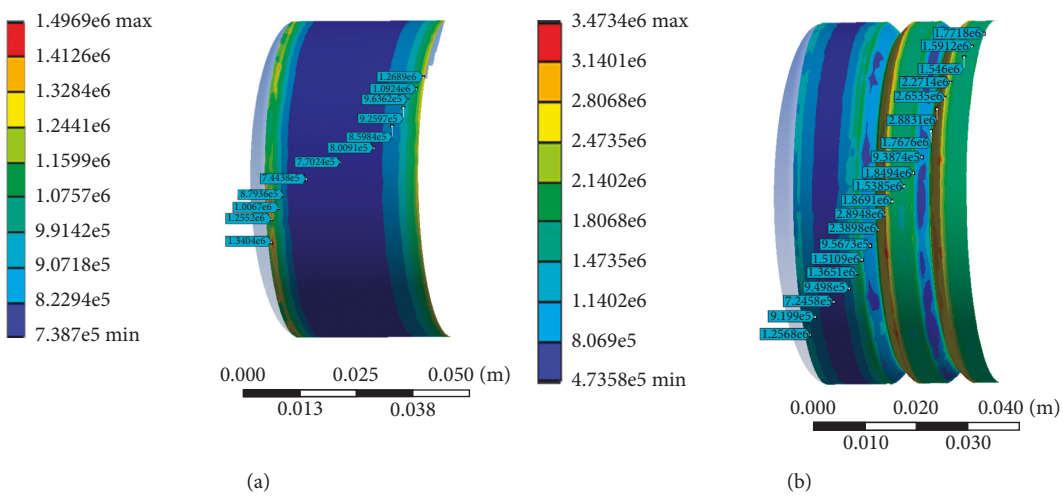

Figure 10: The surface pressures from the lip mouth to the root: (a) standard piston; (b) bionic piston.

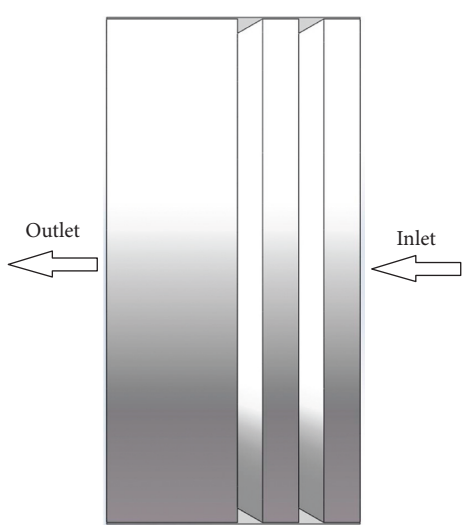

Figure 11: Fluid domain.

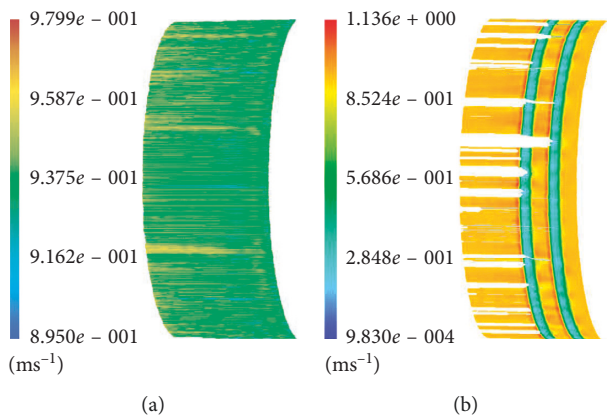

Figure 12: Piston surface leakage streamline: (a) standard piston; (b) bionic piston.

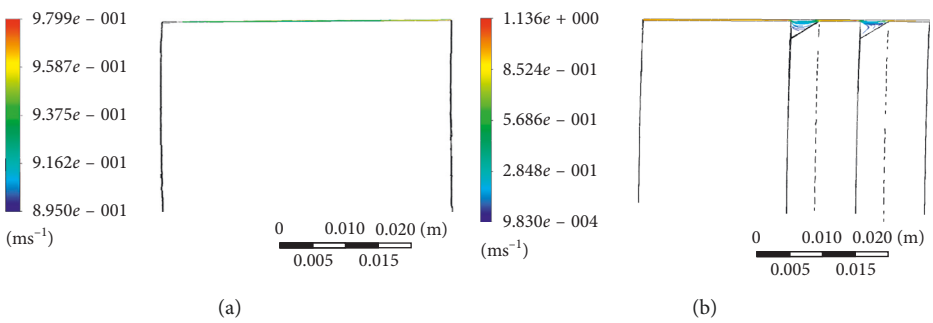

Figure 13: Piston section leakage streamline: (a) standard piston; (b) bionic piston.

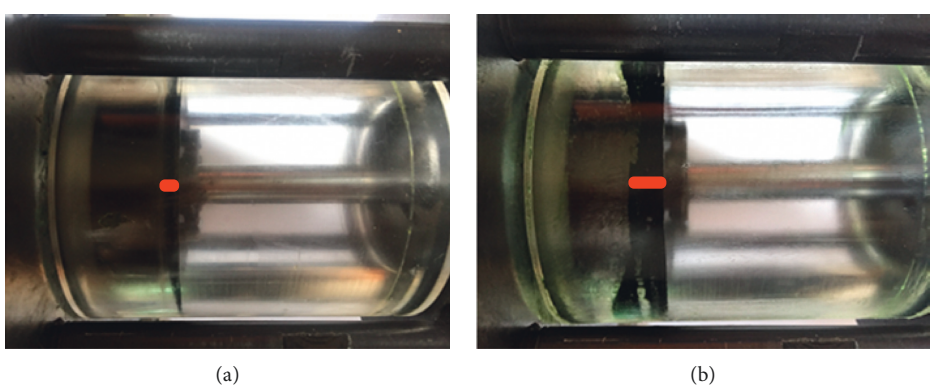

Figure 14: Surface contact of pistons: (a) standard piston; (b) bionic piston. The length of the red line is the contact width.

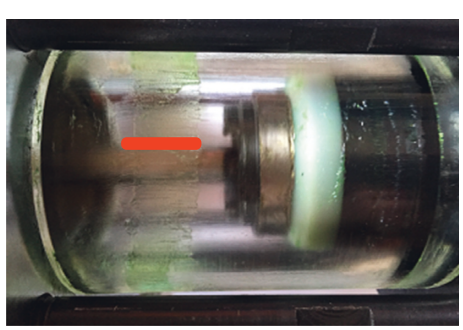

Figure 15: Surface lubrication of pistons. The length of the red line is the oil film width.

uniform oil films after repeated movement, which improved the lubrication conditions and the sealing performance.

The bionic striped structure can improve the sealing performance and prolong the service life of pistons. We would study the pump resistance in order to investigate whether the bionic striped structure could decrease the wear of the piston surface.

Data Availability

All data used to support the findings of this study are available from the corresponding author upon request.

Conflicts of Interest

The authors declare that there are no conflicts of interest regarding the publication of this paper.

Acknowledgments

This project was supported by the National Natural Science Foundation of China (Grant nos. 51375205 and 91748211) and Scientific and Technological Developing Program of Jilin Province (Grant nos. 20160307009GX and 20180101090JC).

References

[1] E. F. Romanenko and V. I. Kolmykov, "Analysis of geological exploration mud pump component wear and damage," *Chemical and Petroleum Engineering*, vol. 49, no. 11-12, pp. 811–815, 2014.

[2] S. Deng, J. Pei, Y. Wang, and B. Liu, "Research on drilling mud pump fault diagnosis based on fusion of acoustic emission and vibration technology," *Insight-Non-Destructive Testing and Condition Monitoring*, vol. 59, no. 8, pp. 415–423, 2017.

[3] T. Piasecki and A. Bejger, "The assessment of the operational suitability of mud pumps on deep water drillships depends on maintenance strategy," *Scientific Journals of the Maritime University of Szczecin*, vol. 46, no. 118, pp. 49–53, 2016.

[4] S. Liu, X. Li, T. Sun, and H. Zhang, "Calculation of the hydraulic extension limit of an extended-reach well with allowance for the power limitations of the available mud pumps," *Chemistry and Technology of Fuels and Oils*, vol. 51, no. 6, pp. 713–718, 2016.

[5] Y. Cao, L. Li, and C. Liu, "Impacts of different land reclamation methods on organic carbon and black carbon in soil in a mine subsided area," *Journal of Resources and Ecology*, vol. 8, no. 2, pp. 191–195, 2017.

[6] L. Cao, Y. Xiao, Z. Wang, Y. Luo, and X. Zhao, "Pressure fluctuation characteristics in the sidewall gaps of a centrifugal dredging pump," *Engineering Computations*, vol. 34, no. 4, pp. 1054–1069, 2017.

[7] M. Yilmaz, N. R. Dhansria, and S. Mujeeba, "An intelligent control approach for oil drilling processes," *Procedia Computer Science*, vol. 6, pp. 106–111, 2011.

[8] Y. Wang, B. Liu, G. Ma et al., "Preparation and property of SiAlON ceramic used on the drilling mud pump cylinder sleeve," *Materials Research Innovations*, vol. 19, no. 9, pp. 310–313, 2016.

[9] A. H. Hoevenaars, M. McGraw, and K. Rittammer, "Preventing centrifuge failures due to voltage distortion on a drilling rig," *IEEE Transactions on Industry Applications*, vol. 52, no. 1, pp. 633–640, 2016.

[10] Z. M. Su, Y. Q. Sun, H. J. Yuan, and J. Y. Guo, "Bayes inference for drilling mud pump piston life," *Applied Mechanics and Materials*, vol. 295-298, pp. 3142–3147, 2013.

[11] H. Yuan, J. Guo, Z. Su et al., "Research on reliability of domestic drilling mud pump piston-cylinder liner friction pair," *China Mechanical Engineering*, vol. 24, no. 11, pp. 1425–1430, 2013.

[12] S.-M. Woo, Y.-H. Kang, and W.-G. Park, "Numerical study of leakage characteristic in labyrinth seals with shapes of rub-groove," *KSFM Journal of Fluid Machinery*, vol. 21, no. 1, pp. 27–33, 2018.

[13] A. Schaller, N. Darvishsefat, and E. Schlücker, "Simulation and experimental investigation of labyrinth seals for reciprocating piston compressors," *Chemical Engineering & Technology*, vol. 41, no. 5, 2018.

[14] T. Fischer, S. Welzenbach, F. Meier et al., "Modeling the rubbing contact in honeycomb seals," *Continuum Mechanics & Thermodynamics*, vol. 30, no. 5, pp. 1–15, 2018.

[15] W. Grabon, W. Koszela, P. Pawlus, and S. Ochwat, "Improving tribological behaviour of piston ring-cylinder liner frictional pair by liner surface texturing," *Tribology International*, vol. 61, no. 61, pp. 102–108, 2013.

[16] A. Ahmed, H. H. Masjuki, M. Varman et al., "An overview of geometrical parameters of surface texturing for piston/cylinder assembly and mechanical seals," *Meccanica*, vol. 51, no. 1, pp. 1–15, 2015.

[17] B. Wu and P. Xi, "Optimal design apply to orthogonal test in piston with bionic groove," in *Proceedings of IEEE International Conference on Mechatronics and Automation*, pp. 805–809, Tianjin, China, August 2014.

[18] X. Cheng, S. Ru, Y. Sun, and Q. Cong, "Wear performance of bionic strip-shaped mud pump pistons," in *Proceedings of the Institution of Mechanical Engineers, Part C: Journal of Mechanical Engineering Science*, vol. 231, no. 21, pp. 4076–4084, 2016.

[19] X. Cheng, T. Gao, S. Ru, and Q. Cong, "Wear performance of bionic dimpled-shape pistons of mud pump," *Advances in Materials Science and Engineering*, vol. 2017, no. 4, pp. 1–11, 2017.

[20] I. Etsion and L. Burstein, "A model for mechanical seals with regular microsurface structure," *Tribology Transactions*, vol. 39, no. 3, pp. 677–683, 1996.

[21] M. Szcz, "Experimental study on the pressure distribution mechanism among stages of the magnetic fluid seal," *IEEE Transactions on Magnetics*, vol. 54, no. 6, pp. 1–7, 2018.

[22] L. Matuszewski, "Multi-stage magnetic-fluid seals for operating in water-life test procedure, test stand and research results," *Polish Maritime Research*, vol. 20, no. 1, pp. 39–47, 2013.

[23] X. Yang, Z. Zhang, and D. Li, "Numerical and experimental study of magnetic fluid seal with large sealing gap and multiple magnetic sources," *Science China Technological Sciences*, vol. 56, no. 11, pp. 2865–2869, 2013.

[24] M. Sun, Z. Y. Zhang, and W. J. Kong, "Design of sealing structure and analysis of the flow field in micro internal combustion swing engine," *Applied Mechanics and Materials*, vol. 670-671, no. 2, pp. 930–935, 2014.

[25] J.-H. Kim, "An experimental study on influence of wearing seal groove shape to performance of the pump," *Journal of Korean Society of Marine Engineering*, vol. 38, no. 3, pp. 285–291, 2014.

[26] M. Yu, I. Hermann, Z. Dai, and N. Gitis, "Mechanical and frictional properties of the elytra of five species of beetles," *Journal of Bionic Engineering*, vol. 10, no. 1, pp. 77–83, 2013.

[27] X. Yang, R. Xia, H. Zhou, L. Guo, and L. Zhang, "Bionic surface design of cemented carbide drill bit," *Science China Technological Sciences*, vol. 59, no. 1, pp. 175–182, 2015.

[28] Z. Han, B. Zhu, M. Yang, S. Niu, H. Song, and J. Zhang, "The effect of the micro-structures on the scorpion surface for improving the anti-erosion performance," *Surface and Coatings Technology*, vol. 313, pp. 143–150, 2017.

[29] G. M. Liu, J. Q. Li, Z. Meng et al., "Feature and the characteristic of sliding resistance reduction of the earthworm's non-smooth surface," *Transactions of the Chinese Society of Agricultural Engineering*, vol. 24, no. 12, pp. 62–65, 2008.

[30] Y. Sun, S. F. Ru, Q. Cong et al., "Life-span test and wear behavior analysis on groove shape bionic piston of mud pump," *Journal of Mechanical Engineering*, vol. 53, no. 21, pp. 95–101, 2017.

[31] C. F. J. Wu and M. Hamada, *Experiments: Planning, Analysis, and Parameter Design Optimization*, John Wiley & Sons, New York, NY, USA, 2000.

[32] J. L. Huang, G. J. Xie, and Z. W. Liu, "Finite element analysis of super-elastic rubber materials based on the Mooney-Rivlin and Yeoh model," *China Rubber/plastics Technology & Equipment*, vol. 34, no. 12, pp. 22–26, 2008.

[33] W. Wang, T. Deng, and S. Zhao, "Determination for material constants of rubber mooney-rivlin model," *Special Purpose Rubber Products*, vol. 25, no. 4, pp. 8–10, 2004.